Food microstructure and fat content affect growth morphology, growth kinetics, and the preferred phase for cell growth of *Listeria monocytogenes* in fish-based model systems

Davy Verheyen[a,b,c], Xiang Ming Xu[d], Marlies Govaert[a,b,c], Maria Baka[a,b,c], Torstein Skåra[e], Jan F. Van Impe[a,b,c]

[a]BioTeC+ - Chemical and Biochemical Process Technology and Control, KU Leuven, Gebroeders de Smetstraat 1, 9000 Gent, Belgium

[b]OPTEC, Optimization in Engineering Center-of-Excellence, KU Leuven, Belgium,

[c]CPMF^2, Flemish Cluster Predictive Microbiology in Foods - www.cpmf2.be

[d]Centre for Organelle Research, University of Stavanger, 4068 Stavanger, Norway

[e]Nofima, P.O. Box 8034, 4068 Stavanger, Norway

davy.verheyen@kuleuven.be, xiang.m.xu@uis.no, marlies.govaert@kuleuven.be, maria.baka@kuleuven.be, torstein.skara@nofima.no, jan.vanimpe@kuleuven.be

Running title: Food microstructure effect on *L. monocytogenes* growth

Declarations of interest: none

Correspondence to:

Prof. J. F. M. Van Impe

Chemical and Biochemical Process Technology and Control (BioTeC+)

Department of Chemical Engineering, KU Leuven

Gebroeders de Smetstraat 1, B-9000 Gent (Belgium)

jan.vanimpe@kuleuven.be

Tel: +32-16-32.14.66

ABSTRACT

Abstract

Food microstructure significantly affects microbial growth dynamics, but knowledge concerning the exact influencing mechanisms at a microscopic scale is limited. The food microstructural influence on *Listeria monocytogenes* (green fluorescent protein strain) growth at 10°C in fish-based food model systems was investigated by Confocal Laser Scanning Microscopy. The model systems had different microstructures, i.e., liquid, xanthan (high-viscosity liquid), aqueous gel, and emulsion and gelled emulsion systems varying in fat content. Bacteria grew as single cells, small aggregates, and micro-colonies of different sizes (based on colony radii (µm), i.e., I: 1.5-5.0, II: 5.0-10.0, III: 10.0-15.0; and IV: ≥15). In the liquid, small aggregates and Size I micro-colonies were predominantly present, while Size II and III micro-colonies were predominant in the xanthan and aqueous gel. Cells in the emulsions and gelled emulsions grew in the aqueous phase and on the fat-water interface. Microbial Adhesion to Solvents Assay demonstrated limited bacterial nonpolar solvent affinities, implying that this behaviour was probably not caused by cell surface hydrophobicity. In systems containing 1 and 5% fat, the largest cell volume was mainly represented by Size I and II micro-colonies, while at 10 and 20% fat, a few Size IV micro-colonies comprised nearly the total cell volume. Microscopic results (concerning, e.g., growth morphology, micro-colony size, inter-colony distances, preferred phase for growth) were related to previously obtained macroscopic growth dynamics in the model systems for a *L. monocytogenes* strain cocktail, leading to more substantiated explanations for the influence of food microstructural aspects on lag phase duration and growth rate.

52

53 **Importance**

54 *Listeria monocytogenes* is one of the most hazardous foodborne pathogens due to the
55 high fatality rate of the disease (i.e., listeriosis). In this study, the growth behaviour of
56 *L. monocytogenes* was investigated at a microscopic scale in food model systems that
57 mimic processed fish products (e.g., fish paté, fish soup), and results were related to
58 macroscopic growth parameters. Many studies have previously focused on the food
59 microstructural influence on microbial growth. The novelty of this work lies in (i) the
60 microscopic investigation of products with a complex composition and/or structure
61 using Confocal Laser Scanning Microscopy, and (ii) the direct link to the macroscopic
62 level. Growth behaviour (i.e., concerning bacterial growth morphology and preferred
63 phase for growth) was more complex than assumed in common macroscopic studies.
64 Consequently, the effectiveness of industrial antimicrobial food preservation
65 technologies (e.g., thermal processing) might be overestimated for certain products,
66 which may have critical food safety implications.

67

68

69 **Keywords:** Confocal Laser Scanning Microscopy, *Listeria monocytogenes*, fat
70 content, growth morphology, micro-colony size.

71

1 INTRODUCTION

In recent years, global fish product consumption has increased significantly (1-3). Fish products are known to be beneficial for human health, being an important source of high-quality proteins, vitamins, minerals, and omega-3 fatty acids (4-6). However, contamination with foodborne pathogens is common in fish products, as illustrated by the percentage of foodborne outbreaks caused by products of this food category, e.g., 5.4% in 2016 (7). The bacterium *Listeria monocytogenes*, causing listeriosis, has been detected in fish products on a regular basis since 1987 (7-9). Listeriosis is an illness with a mortality rate of more than 20% (10), with clinical features ranging from mild influenza-like illness to invasive diseases like meningitis and meningoencephalitis (11).

In predictive microbiology, the effect of food processing, distribution and storage operations on microbiological safety is evaluated by means of mathematical models that describe microbial responses to environmental conditions (12, 13). Since predictive models are traditionally developed based on experimental data from homogeneously well-mixed broth media, in essence ignoring food microstructure and composition, model accuracy for the behaviour of microorganisms in more structured food products is often limited (14-16). Food microstructure encompasses the spatial arrangement of the various structural elements (e.g., water and oil droplets, gas cells, particles, granules, strands, crystals, micelles, and interfaces) of a food product and their interactions (17). Microbial dynamics are affected by a plethora of food microstructural aspects, e.g., physical constraints on microbial mobility (18-20), the presence of fat in the food matrix (21, 22), the nature of the food matrix (i.e., viscous

or gelled) (22), and diffusion of oxygen, water, nutrients, preservatives, and metabolites (23-27).

One approach that allows inclusion of the food microstructural influence into predictive models, is to conduct microbiological experiments in food model systems with various microstructures (28-31). Wilson et al. (26) defined five categories of food microstructures, i.e., liquids, emulsions, aqueous gels, gelled emulsions, and surfaces. Based on this classification, Baka et al. (29) investigated the influence of food microstructure on growth dynamics of *L. monocytogenes* at suboptimal temperatures using model systems based on processed fish products. However, apart from the variation in microstructure among those model systems, there was also variation in compositional and physicochemical factors. These unwanted variations were caused by the presence or absence of fat and gelling agents in some of the systems, a consequence of developing representative model systems for each microstructure. For this reason, Verheyen et al. (31) developed model systems with various microstructures among which the microstructural effect was isolated by means of minimal variation in compositional and physicochemical aspects. The set of model systems consisted of three viscous systems and two gelled systems, i.e., (i) a liquid system, (ii) xanthan, a more viscous liquid system containing a small concentration of xanthan gum, (iii) an emulsion, (iv) an aqueous gel, and (v) a gelled emulsion, respectively. These model systems were used to investigate the effect of food microstructure on growth dynamics of *L. monocytogenes* at suboptimal temperatures, i.e., 4 and 10°C (22). The growth morphology of the cells (i.e., planktonic cells, submerged colonies, or surface colonies), the nature of the food matrix (i.e., viscous or gelled), and the presence of fat droplets were reported to exert

a significant influence on the parameters of the growth model of Baranyi and Roberts (32). Since the study of Verheyen et al. (22) relied solely on macroscopic growth experiments, the underlying mechanisms have mostly been left unravelled. More specifically, apart from a visual inspection during the macroscopic growth experiments, a detailed investigation of the growth morphology in which *L. monocytogenes* appeared in the different model systems was not conducted. Quantification of colony sizes could lead to more insight in the observed differences in macroscopic growth dynamics. Colonies can either be classified as micro-colonies (i.e., radius < 200 µm) or macro-colonies (i.e., radius > 200 µm). While micro-colony growth largely resembles planktonic growth, macro-colony growth is slower, due to the presence of pH gradients and diffusion limitations around and inside the colonies (33). Additionally, single cells can also cluster together and form small aggregates (i.e., radius < 1.5 µm) which cannot be considered as full-fledged micro-colonies (33-37). Another finding of the study was the growth-promoting effect of a small percentage of fat droplets in the model system matrix for which the causes remained unknown. More fundamental research towards these phenomena at a microscopic scale will lead to increased insight into the influence of food microstructure on microbial growth dynamics.

While food products generally consist of different phases, most microbiological studies are only conducted at a macroscopic scale, ignoring heterogeneity. In order to characterise the behaviour of microorganisms in a complex food product, more advanced micro-scale measurement techniques are therefore necessary (38). Confocal Laser Scanning Microscopy (CLSM) is a non-destructive technique which has several advantages compared to conventional light microscopy, e.g., the applicability of

fluorescent probes to stain and visualise different components, the possibility of using relatively thick samples due to the removal of out-of-focus light, and the possibility of creating 3D images by using a sequence of optical sections at different sample heights (39).

The aim of this study was to investigate the effect of food microstructure on *L. monocytogenes* growth dynamics at the microscopic level and relate the obtained results to findings at the macroscopic level. In order to compare microscopic and macroscopic observations, the bacteria were grown inside fish-based food model systems at 10°C, analogous to the macroscopic growth experiments conducted by Verheyen et al. (22). Model system composition was based on processed fish products (e.g., fish soup, surimi, and fish paté) and the microstructure was simulated by including the major food microstructural aspects of those products (e.g., a visco-elastic matrix or fat droplets). While a cocktail of three *L. monocytogenes* strains isolated from fish-based food products was used in the above-mentioned macroscopic study, a Green Fluorescent Protein (GFP) *L. monocytogenes* strain was used in the current study in order to facilitate CLSM experiments. Confocal images were used to study the growth morphology of the cells in each model system and the growth morphology was characterised by means of the number and volume distribution of single cells, small aggregates, and micro-colonies with various sizes. For the emulsion and gelled emulsion model systems, the preferred phase (i.e., aqueous phase, fat phase, or the interface) for *L. monocytogenes* growth was investigated using systems with various fat levels (i.e., 1, 5, 10, and 20%). As a possible explanation for the affinity of the cells for a certain phase, hydrophobicity of the cells was quantified using the Microbial Adhesion To Solvents (MATS) assay (40). The MATS assay was

171 conducted for both the GFP strain and the *L. monocytogenes* strain cocktail used for
172 the macroscopic growth experiments of Verheyen et al. (22), enabling an improved
173 comparison of microscopic and macroscopic results.
174

2 RESULTS

2.1 Confocal Laser Scanning Microscopy

Confocal Laser Scanning Microscopy (CLSM) images were used to visualise the growth behaviour of the selected *L. monocytogenes* (GFP) strain in the different model systems after 14 days of incubation at 10°C. Bacterial cells were visualised in green and fat droplets (if relevant) in orange. Cell cluster sizes were quantified and subsequently classified in six categories, i.e., single cells, small aggregates, and micro-colonies of four different sizes. Since interpreting linear size parameters is more straightforward than interpreting squared or cubic size parameters (41), cell cluster size was expressed in terms of the equivalent spherical radius (r_s) based on the measured cluster volumes. This method is similar to the protocol of Jung and Lee (42), in which the equivalent circular colony radius was calculated based on the colony surface. Micro-colonies were defined as cell clusters for which $r_s \geq 1.5$ µm, and were further divided in four different size categories: Size I (1.5 µm $\leq r_s <$5.0 µm), Size II (5.0 µm $\leq r_s <$ 10.0 µm), Size III (10.0 µm $\leq r_s <$ 15.0 µm), and Size IV ($r_s \geq$ 15 µm). Micro-colonies with sizes ranging between 1.5 and 200 µm are reported in literature (33); the four micro-colony size subcategories in the current study were defined based on the experimental micro-colony sizes (as computed from the CLSM images) to enable a balanced micro-colony size distribution. Since *L. monocytogenes* cells are rod-shaped, measuring approximately 0.5 – 2.0 µm in length and 0.4 – 0.5 µm in width (43), cell clusters for which $r_s <$ 1.5 µm were further categorised based on the height of a cylinder with equivalent volume and a diameter of 0.5 µm (i.e., the largest possible width of a single rod-shaped cell). Clusters for which this cylindrical height was smaller than or equal to 2 µm were categorised as single cells, while larger clusters were categorised as small aggregates. For the different model systems, Figure

1 and 2 show the size distribution of the cell clusters in the aforementioned categories by means of the number and volume distribution, respectively.

Figure 3 represents the distribution of the selected GFP *L. monocytogenes* strain in the three different model systems without fat, i.e., liquid, xanthan, and aqueous gel. Figures 1 and 2 illustrate that *L. monocytogenes* mainly grew as small aggregates and micro-colonies in these model systems. In the liquid model system (Figure 3A), *L. monocytogenes* grew mainly as small aggregates and Size I micro-colonies. While the number of small aggregates was higher than the number of micro-colonies, most of the volume was taken in by the micro-colonies. In the xanthan system (Figure 3B), a large number of small aggregates and Size I micro-colonies were present. However, the two larger micro-colonies of Size II (i.e., r_s of 8.1) and Size III (i.e., r_s of 13.9 µm) accounted for 95% of the total volume of *L. monocytogenes* in xanthan. In the aqueous gel (Figure 3C), the cells were, in absolute numbers, rather equally divided between small aggregates and Size I, II, and III micro-colonies, while most of the cell volume was represented by Size II and III micro-colonies.

Figure 4 illustrates the growth behaviour of *L. monocytogenes* in the emulsion and gelled emulsion model system containing 1% fat. In both systems, fat droplets with a diameter of approximately 1 µm were present, and *L. monocytogenes* grew in the space among these fat droplets. However, the green and yellow areas that were observed on the outside of the orange areas indicated that the bacterial cells also grew around the fat droplets on the fat-water interface. In the emulsion containing 1% fat (Figure 4A), the cells mainly grew as small aggregates and Size I micro-colonies, with the latter representing the largest cell volume. In the gelled emulsion containing 1%

fat (Figure 4B), a similar growth behaviour was observed, although Size II micro-colonies also represented 11% of the cell volume.

The growth of the GFP *L. monocytogenes* strain in the model systems with higher fat content (i.e., 5, 10, and 20%) is illustrated in Figure 5 and Figure 6, for the emulsions and gelled emulsions, respectively. With increasing fat content, bacterial growth on the fat-water interface was dominant over growth in the aqueous phase among the fat droplets. Concerning number and volume distribution of cells, growth behaviour was relatively similar in emulsions and gelled emulsions with equal fat content. In systems containing 5% fat, most cell clusters appeared as small aggregates and Size I micro-colonies, with the latter category representing the largest volume percentage. In the emulsions and gelled emulsions containing 10 and 20% fat, small aggregates and Size I micro-colonies were the most prominent in absolute numbers, while smaller percentages of Size II and IV micro-colonies were also seen. However, these Size IV micro-colonies (i.e., r_s of 30.6, 39.4, 16.3, 27.5, and 37.2 µm) represented between 90 and 100% of the total cell volume. These relatively large micro-colonies seem to have been formed by the connection of micro-colonies on different fat droplets, as can be observed in Figure 5 and Figure 6 (B and C).

2.2 MATS assay

Table 1 shows the results of the MATS assay for the GFP strain, the strain cocktail used for the macroscopic growth experiments by Verheyen et al. (22), and the three separate strains of the cocktail (i.e., LMG 23773, LMG 23774, and LMG 26484). In general, affinities for the polar solvent (i.e., diethyl ether) were higher than for the nonpolar solvent (hexane). The affinity for diethyl ether was significantly higher for

LMG 23773 than for the other strains. The highest affinities for hexane were observed for LMG 23773 and the GFP strain. For each strain, the affinity to the polar solvent was also higher than the affinity to the nonpolar solvent.

3 DISCUSSION

3.1 Growth morphology

Verheyen et al. (22, 31) made a number of assumptions concerning the growth morphology of the *L. monocytogenes* strain cocktail (consisting of LMG 23773, LMG 23774, and LMG 26484) in the investigated fish-based model systems with various microstructures, i.e., liquid, xanthan, aqueous gel, emulsion (1% fat), and gelled emulsion (1% fat). First of all, it was assumed that *L. monocytogenes* grew as single cells in the liquid system, although potential cell sedimentation due to the static nature of the growth experiments was also suggested. Secondly, visual inspection during the macroscopic growth experiments indicated the occurrence of colony growth in the xanthan model system, probably caused by the higher viscosity in comparison to the liquid system. Since the viscosities of the xanthan and emulsion model system containing 1% fat were rather similar, it was assumed that colony growth would also be present in the emulsion model system. Furthermore, it was assumed that *L. monocytogenes* grew as colonies in the aqueous gel and the gelled emulsion containing 1% fat. It is important to mention that the distinction between micro- or macro-colonies could not be made based on the macroscopic growth experiments. The current study shows that colony growth in the model systems could in fact be classified as micro-colony growth.

The assumption of the predominant presence of single cells in the liquid system (Figure 3A) was not confirmed in the current study, since *L. monocytogenes* mainly grew as small aggregates and Size I micro-colonies (i.e., 1.5 µm $\leq r_s <$ 5 µm). In this regard, bacteria are known to form small aggregates and more dense clusters when grown in liquid systems, especially at static conditions (44). The sedimentation of

cells during the 14 days of incubation at 10°C is a plausible explanation for the presence of small aggregates and micro-colonies (45, 46). For the xanthan system (Figure 3B) and the emulsion containing 1% fat (Figure 4A), the assumption of micro-colony growth was confirmed, as the largest cell volume was represented by micro-colonies. However, the situation was more complex than assumed, since a large number of small aggregates and some single cells were also present in these two systems. Furthermore, micro-colonies grew to significantly larger sizes in the xanthan system than in the emulsion system, indicating that, even at a low fat content of 1%, micro-colony size is constrained by the presence of fat droplets. This finding contradicts previous studies on bacterial growth in oil-in-water emulsions for which the main conclusion was that planktonic growth is predominant in emulsions with fat content lower than 80% (21, 26). Not only did the cells grow as small aggregates and small micro-colonies, but their colony size was also limited by a fat content significantly lower than 80%. For the aqueous gel (Figure 3C), the assumption of micro-colony growth was also mostly confirmed. Although a substantial number of small aggregates was also detected in the system, most of the cell volume was represented by micro-colonies. In the gelled emulsion containing 1% fat (Figure 4B), the assumption of micro-colony growth was also mostly confirmed, again in addition to a large number of small aggregates which only represented a limited percentage of the total cell volume. Micro-colonies in the gelled emulsion were generally smaller than in the aqueous gel, probably due to the space limitations caused by the presence of the fat droplets.

Inter-colony distances of *L. monocytogenes* micro-colonies can also be investigated in Figures 3-6. The inoculation level of the growth experiments conducted in the current

study and by Verheyen et al. (22) was 10^2 CFU/mL. This low inoculation level has been reported to lead to growth of large micro-colonies, far apart from each other (i.e., 1.5-5.0 mm) with no inter-colony interactions (47). Inter-colony distances of the aforementioned order of magnitude could be present among the larger micro-colonies in the xanthan system, since only one Size III micro-colony (i.e., 13.9 µm) was visible in Figure 3B, implying that more distant large micro-colonies could be located at 1.5-5.0 mm of the visible micro-colony. The absence of these larger inter-colony distances in the other model systems was probably related to the limited mobility of the bacterial cells in comparison to the xanthan system. Possible causes for this limited mobility include (i) sedimentation of cells in the liquid system, (ii) immobilisation of cells in the aqueous gel and gelled emulsion, and (iii) the presence of fat droplets in the emulsion and gelled emulsion.

In general, the growth morphologies of *L. monocytogenes* in the different model systems as assumed by Verheyen et al. (22, 31) for the macroscopic growth experiments, were more simplistic than those observed in the microscopic images in the current study. *L. monocytogenes* often appeared as a combination of single cells, small aggregates and micro-colonies varying in size, in contrast to the more simple classification that was previously assumed, i.e., growth of single cells in the liquid system and submerged micro-colony growth in the xanthan, emulsion system, aqueous gel, and gelled emulsion system.

3.2 Preferred phase for cell growth

Verheyen et al. (22, 31) assumed that the aqueous phase was the preferred phase for cell growth in the emulsion and gelled emulsion systems. However, Figures 4-6

illustrate that *L. monocytogenes* showed a preference for growth around the fat droplets on the fat-water interface, a trend which became more evident in systems with higher fat content (i.e., 5, 10, and 20%). Although previous studies have reported that bacteria grow exclusively in the aqueous phase of oil-in-water emulsions (e.g., 21, 48, 49), some bacteria have been reported to have a preference for the fat-water interface in emulsion systems, e.g., demulsifying bacteria such as *Alcaligenes* sp. S-XJ-1 (50-52), and different bacteria in Emmental cheese (53). Therefore, the preference of *L. monocytogenes* to grow on the fat-water interface, as observed in this study, is not a totally isolated case. In certain conditions, bacteria can adhere to oil droplets if their cell surface is (partially) hydrophobic or exhibits specific adherence features such as pili, fimbriae, and flagella (54, 55). *L. monocytogenes* cells are known to possess flagella at temperatures below 30°C (56, 57), promoting adhesion to inert solid surfaces such as polystyrene and stainless steel (58, 59). However, flagella-induced *L. monocytogenes* adhesion to fat droplets has, to the best knowledge of the authors, thus far not been reported. Therefore, cell surface hydrophobicity was investigated (i.e., by means of the MATS assay) as a possible driving force behind the preference of *L. monocytogenes* to grow around the fat droplets in the current study. Since cell surface hydrophobicity of *L. monocytogenes* is strain-dependent (60), the MATS assay was conducted for the selected GFP *L. monocytogenes* strain, the *L. monocytogenes* strain cocktail, and for the three separate strains of the cocktail used in the macroscopic growth experiments (22), in order to check transferability of findings to the macroscopic scale.

No statistically significant differences were observed between affinities to the polar solvent of the GFP strain and the strain cocktail (and each separate strain of the

cocktail except LMG 23773), while the affinity to the nonpolar solvent was significantly higher for the GFP strain than for the strain cocktail. However, these statistical differences for the affinity to the nonpolar solvent were mainly due to the negative value obtained for the strain cocktail. The occurrence of negative numbers was caused by small measurement variances (i.e., the optical density of the mixed sample being slightly higher than the optical density of the original cell suspension), meaning that negative values can be assumed to be equal to zero. In addition, only one of the three strains of the strain cocktail (i.e., LMG 23774) exhibited a significantly lower affinity to the nonpolar solvent than the GFP strain, also due to the negative value which was obtained for this strain. Hence, it is reasonable to assume that both the polar and nonpolar affinity of the GFP strain and the strain cocktail were similar.

The adhesion of the different strains ranged approximately from 30 to 50% for the polar solvent, and from -5 to 11% for the nonpolar solvent. The combination of both a polar and nonpolar affinity for the investigated strains could explain the tendency of the cells to grow on the fat-water interface. This would mean that the partial affinity to the nonpolar fat-phase starts to play a more important role when a decreased growth space is available in the aqueous phase (i.e., in systems with a higher fat content). However, in other studies (60-63), *L. monocytogenes* strains exhibited considerably higher affinities to nonpolar solvents (i.e., up to 96%) than in the current study. In addition, significantly higher affinities to polar solvents than to nonpolar solvents were observed in those studies, an opposite trend as compared to the current study. Nevertheless, while cell surfaces in the aforementioned studies exhibited rather hydrophobic properties, the cells still adhered preferably to polar surfaces (e.g., stainless steel). Even though the comparison of cell surface hydrophobicity among

different studies is not straightforward (due to the influence of e.g., the physiological state of the cells, nutrient concentration, growth temperature, and growth phase (62-65)), it can be suggested that mechanisms other than cell surface hydrophobicity were more dominant causes for the preferred growth around the fat droplets in the current study. Future studies could focus on elucidating the exact causing mechanisms of the phenomenon by investigating e.g., gene expression of *L. monocytogenes* in the presence of fat droplets, bacterial motility, and the presence/absence of specific adherence features such as pili, fimbriae, and flagella.

3.3 Comparison to macroscopic growth experiments

Verheyen et al. (22) investigated the influence of food microstructure on the growth dynamics of the *L. monocytogenes* strain cocktail at 4 and 10°C at a macroscopic scale, using the liquid, xanthan, aqueous gel, emulsion (1% fat), and gelled emulsion (1% fat) model systems. An overview of macroscopic growth parameters (i.e., the lag phase λ and the maximum specific growth rate μ_{max}) obtained in the different model systems for growth at 4 and 10°C is provided in Table 2. Since the main objective of the macroscopic study was to isolate the microstructural effect on growth dynamics, macroscopic growth parameters could only be effectively compared among model systems which only differed in the form of a single isolated microstructural aspect. In this regard, a comparison of planktonic cells in the liquid system and submerged micro-colonies in the xanthan system demonstrated that submerged micro-colonies of *L. monocytogenes* grew faster (i.e., similar λ, higher μ_{max}) than planktonic cells, at least at static conditions (i.e., cultures which were not shaken). Furthermore, growth was faster (i.e., similar λ, higher μ_{max}) in viscous systems than in gelled systems, as illustrated by the higher μ_{max} in the xanthan system as compared to the aqueous gel,

and in the emulsion system as compared to gelled emulsion. Finally, fat droplets promoted growth (i.e., shorter λ, higher μ_{max}) at 4°C, illustrated by comparing growth in the xanthan system and the emulsion, and in the aqueous gel and the gelled emulsion. Results from the current study can be used to explain some of the findings from these macroscopic growth experiments, although possible differences in growth behaviour between the *L. monocytogenes* strain cocktail and the GFP strain should be taken into account. In addition, assumptions made in the macroscopic study concerning *L. monocytogenes* growth morphology in the different model systems were proven too simplistic, as has been demonstrated in section 3.1 "Growth morphology". The complex behaviour concerning the preferred phase for cell growth in the emulsion and gelled emulsion systems, as has been discussed in section 3.2 "Preferred phase for cell growth", could also not be taken into account during the macroscopic growth experiments. Hence, the conclusions from Verheyen et al. (22) concerning the influence of bacterial growth morphology and the presence of fat droplets on *L. monocytogenes* growth dynamics should be interpreted critically.

In order to investigate the influence of *L. monocytogenes* growth morphology on microbial dynamics, macroscopic growth parameters in the liquid and xanthan system were compared. At 4°C, no significant differences in μ_{max} were observed between the two systems, while λ was longer in the liquid system. At 10°C, the maximum specific growth rate μ_{max} was higher in the xanthan system, while no significant differences were observed in λ. It was suggested that cells in the liquid model system might have sedimented due to the static nature (i.e., the tubes were not shaken during incubation) of the experiments. Therefore, oxygen availability would be lower for the cells in the liquid than in the xanthan system (45, 46). This assumption of sedimentation could be

valid, since the current study shows that the number of small aggregates and small (i.e., Size I) micro-colonies in the liquid system was considerably higher than the number of single cells. Nevertheless, since the number of single cells were similar in the liquid and xanthan system, differences in macroscopic growth parameters were probably mainly caused by the higher viscosity of the xanthan system, rather than by differences in bacterial growth morphology (i.e., between single cells and micro-colonies).

The influence of the nature of the food matrix (i.e., viscous or gelled) on growth dynamics was investigated by comparing macroscopic growth parameters among (i) the xanthan system and the aqueous gel, and (ii) the emulsion and the gelled emulsion containing 1% fat. A higher μ_{max} was observed in viscous systems than in gelled systems at 4 and 10°C, which could be explained by the enhanced nutrient, oxygen and metabolite diffusion in the viscous systems. Based on the results of the current study, the difference in separation distance between the micro-colonies in the viscous and gelled systems could be another possible explanation for the differences in μ_{max}, at least when comparing the xanthan system and the aqueous gel. Figure 3 illustrates that Size III micro-colonies (i.e., 10.0 µm $\leq r_s <$ 15.0 µm) in the aqueous gel were situated more closely together than those in the xanthan system. Since colony interactions from close spatial distribution of colonies occur up to separation distances of 1400 to 2000 µm (66, 67), the smaller separation distance between the micro-colonies in the aqueous gel might also be an explanation for the higher μ_{max} in the xanthan system. Single cells, small aggregates, and Size I and II micro-colonies, however, were also located close to each other and to the Size III micro-colonies in the xanthan system, possibly also resulting in local depletion of nutrients and oxygen.

455 In addition, the growth behaviour of colonies depends on the colony size. Micro-
456 colony growth largely resembles planktonic growth, while macro-colony growth is
457 slower than planktonic growth due to the presence of pH gradients and diffusion
458 limitations around and inside the colonies (33). Since no macro-colonies were
459 observed in any of the model systems, enhanced nutrient, oxygen and metabolite
460 diffusion in the viscous systems as compared to the gelled systems remains the most
461 probable explanation for the higher μ_{max} in the viscous systems.
462
463 The influence of fat droplets on *L. monocytogenes* growth was investigated by
464 comparing macroscopic growth parameters between (i) the xanthan system and the
465 emulsion containing 1% fat, and (ii) the aqueous gel and the gelled emulsion
466 containing 1% fat. Results showed that the presence of fat droplets was beneficial for
467 the growth of *L. monocytogenes* (i.e., shorter λ and higher μ_{max}), although only at 4°C.
468 Therefore, it was suggested that the presence of fat acts as a cryoprotective agent for
469 *L. monocytogenes* growth, as concluded by Baka et al. (29). This behaviour might be
470 explained by the tendency of the cells to grow around the fat droplets, as can be
471 observed in Figure 4. Figure 5 and 6 illustrate that the affinity of the cells for the fat
472 droplets seems to increase with increasing fat content. In general, a complex
473 relationship between *L. monocytogenes* growth temperature and fat presence has been
474 reported in literature (22, 29), which could also be related to the preferred phase for
475 cell growth. Future studies could combine macroscopic growth experiments and
476 CLSM to investigate *L. monocytogenes* at different temperatures in emulsion and/or
477 gelled emulsions systems with different fat content in order to get more insight into
478 the cell growth on the fat-water interface and the resulting influence on macroscopic
479 growth parameters. Similar to the concluding remarks of Section 3.2 “Preferred phase

480 for cell growth", the influence of bacterial motility and the presence/absence of
481 flagella on macroscopic growth parameters could also be investigated.
482
483 The findings of the current study entail significant implications for the microbial
484 safety of processed fish-based food products, and food safety in general. In literature,
485 assumptions concerning microbial growth morphology tend to be rather simplistic, as
486 three different situations are normally distinguished based on the specific food
487 microstructure, i.e., (i) planktonic growth in liquid products, (ii) submerged colony
488 growth in gelled products, and (iii) surface colony growth on food surfaces (26, 68).
489 In the current study, it was demonstrated that this classification does not always
490 adequately describe real microbial behaviour, not even in products with a
491 homogeneous microstructure. In liquid products (e.g., the liquid and xanthan model
492 system in this study), a combination of single cells, small aggregates, and micro-
493 colonies can be present, with the distribution of the bacteria over this spectrum
494 probably being dependent on the viscosity and potential shaking of the product. While
495 the presence of small aggregates and micro-colonies exerts no significant influence on
496 microbial growth dynamics (33), microbial inactivation treatments (e.g., thermal
497 inactivation, cold atmospheric plasma, antimicrobial compounds) are often less
498 effective when such cell clusters are present in foods (69-71). As a consequence, the
499 inactivation efficiency of preservation processes designed for liquid/viscous food
500 products could be lower than estimated when cells do not exclusively grow in
501 planktonic form. With the model systems in the current study being based on
502 processed fish-based food products, such products containing a viscous aqueous phase
503 (e.g., fish soup or certain fish curries) are potentially affected by the aforementioned
504 consequences. In addition, bacteria growing on the fat-water interface (i.e., around fat

505 droplets) in emulsion or gelled emulsion type food products could exhibit an
506 increased growth potential and inactivation resistance as compared to bacteria which
507 solely grow in the aqueous phase of those products. With the applicability of the
508 model systems of the current study in mind, these risks are especially relevant for
509 processed fish products containing 1 to 20% fat (e.g., fish paté or fish sausage) (72-
510 74).

4 MATERIALS AND METHODS

4.1 Microorganism and preculture conditions

The GFP *L. monocytogenes* ScottA strain harbouring the plasmid pNF8 (75) was kindly donated by Prof. Tine Rask Licht (National Food Institute, Technical University of Denmark). In order to maintain the structural stability of the constructed fluorescent plasmids, 10 µg/mL of Erythromycin (Sigma Aldrich, MO, USA) and 100 µg/mL of Nalidixic acid (Sigma Aldrich, MO, USA) were added to all growth media. Stock cultures were stored in Microbank (Pro-Lab Diagnostics, ON, Canada) at -80°C. One Microbank bead was transferred to 20 mL of Brain Heart Infusion Broth (BHI, VWR International, Leuven, Belgium) in a 50 mL Erlenmeyer flask, and incubated at 30°C for 24 h at static conditions. Afterwards, 20 µL of the stationary-phase culture was inoculated into 20 mL of fresh BHI and incubated for 24 h under the same conditions, resulting in stationary-phase cultures with a cell density of approximately 10^9 CFU/mL.

L. monocytogenes strains LMG 23773, LMG 23774 (both isolated from smoked salmon), and LMG 26484 (isolated from tuna salad) were acquired from the BCCM/LMG bacteria collection (Ghent University, Belgium). Stock cultures were stored at -80°C in a mixture of 80% (v/v) BHI broth and 20% (v/v) glycerol (Acros Organics, NJ, USA). For each strain, fresh purity plates were prepared by spreading a loopful of the stock culture onto a BHI Agar plate (1.4% (w/v), Agar Technical No3, Oxoid Ltd., Basingstoke, UK). After incubation at 30°C for 24 h, one colony from each purity plate was transferred to separate Erlenmeyer flasks containing 20 mL of BHI, after which the same procedure as for the GFP strain was followed. To prepare the strain cocktail, 10 mL from each culture (i.e., one of each strain) was collected

under aseptic conditions and mixed, leading to a stationary-phase mixed culture with a cell density of approximately 10^9 CFU/mL.

4.2 Model system preparation and inoculation

Fish-based model systems with different microstructures were prepared according to the protocol of Verheyen et al. (31). The composition of the model systems was based on processed fish products (e.g., fish soup, surimi, and fish paté), while major food microstructural aspects of such products were also included (e.g., a visco-elastic matrix or fat droplets). A more detailed description of the model systems, as well as a detailed preparation protocol, is provided in Verheyen et al. (31). Briefly, the model systems were classified into five categories, i.e., liquid, xanthan (a more viscous liquid system containing a small concentration of xanthan gum), emulsion (oil-in-water), aqueous gel, and gelled emulsion. The liquid, xanthan and emulsion system were classified as viscous systems, while the aqueous gel and gelled emulsion were classified as gelled systems. In order to study the effect of fat content, emulsion and gelled emulsion systems containing different concentrations of sunflower oil were used, i.e., 1, 5, 10, and 20%. Prior to the pasteurisation step (i.e., heating for 2 h at 80°C while being continuously stirred at 400 rpm) of the fat solutions (as described in Verheyen et al. (31)), Nile Red (Sigma Aldrich, MO, USA) was added to the fat solutions in powdered form to a concentration of 3 µg per gram of fat. After the addition of 10 µg/mL of Erythromycin and 100 µg/mL of Nalidixic acid, model systems were homogeneously inoculated with the GFP *L. monocytogenes* strain to a cell density of 10^2 CFU/mL, using the inoculation procedure as described in Verheyen et al. (22). Inoculated systems were distributed over 35 mm diameter glass bottom dishes with a 27 mm glass viewing area (Nunc, Thermo Fisher Scientific, Waltham,

MA, USA) suitable for confocal image analysis (4 mL per dish). Prior to CLSM imaging, model systems were incubated at 10°C for 14 days, resulting in early stationary phase cells with a cell density of approximately 10^8-10^9 CFU/mL (22).

4.3 Confocal Laser Scanning Microscopy image acquisition

Microscopic 3D-images were recorded using the z-series dissection function of an A1R Confocal Laser Scanning Microscope (Nikon, Tokyo, Japan) at a 60× magnification (water immersion objective). Excitation wavelengths were 408 and 561 nm for the GFP strain and Nile Red, respectively. The recorded emission ranges were 500 – 550 nm and 570 – 620 nm. Images were processed using NIS-Elements C imaging software (Nikon, Tokyo, Japan). All experiments were independently performed in duplicate and multiple images were taken for each experiment. The images that were chosen were those that were the most representative and clear for the observed phenomena.

4.4 Cell cluster size determination

BioImageXD software (76) was used to calculate the volume of cell clusters (i.e., single cells, small aggregates, and micro-colonies) on the confocal images. 3D images were constructed in the software by importing separate TIFF-files for each z-slice of the CLSM images. Noise was filtered using the "mean" function, with x, y, z values of 3. Images were (manually) thresholded in order to acquire similar cell cluster distributions as for the original CLSM images. All green areas were separated into segmented objects with identifying colours using the "connected component labelling" function and the volume of the segmented objects was quantified. The equivalent spherical radius (r_s) of all objects was calculated as the radius of a sphere

with a volume equal to the object. Similarly, the equivalent cylindrical height (h_c) of the object was calculated, assuming that the object was a cylinder with a diameter of 0.5 µm. Objects were classified as micro-colonies ($r_s \geq 1.5$ µm), small aggregates ($r_s <$ 1.5 µm and $h_c > 2$ µm), and single cells ($r_s < 1.5$ µm and $h_c \leq 2$ µm). Micro-colonies were further classified in four different size categories: Size I (1.5 µm $\leq r_s <$5.0 µm), Size II (5.0 µm $\leq r_s <$ 10.0 µm), Size III (10.0 µm $\leq r_s <$ 15.0 µm), and Size IV ($r_s \geq$ 15 µm). These size subcategory ranges were defined based on the experimental micro-colony sizes computed from the CLSM images in order to enable a balanced micro-colony size distribution. For each model system, number and volume distributions were calculated to quantify the distribution of cell clusters over the six different categories.

4.5 Microbial adhesion to solvent (MATS) assay

The MATS assay was performed based on the protocols of Bellon-Fontaine et al. (40) and Takahashi et al. (60). Hydrophobicity of bacterial surfaces was assessed by comparing affinities to diethyl ether (i.e., a polar solvent) and hexane (i.e., a nonpolar solvent having intermolecular attraction comparable to that of diethyl ether). Precultures of the four different *L. monocytogenes* strains (i.e., LMG 23773, LMG 23774, LMG 26484, and the GFP strain) and the strain cocktail consisting of LMG 23773, LMG 23774, LMG 26484 were prepared and grown as described in Section 4.1 “Microorganism and preculture conditions”. The cells were washed twice with a NaCl solution of 0.90% (w/v), centrifuging at 18,500 × g for 10 min at 4°C. In order to reach an initial optical density of approximately 0.400 at 400 nm, the cells were 2.5-fold diluted with the NaCl solution. After measuring the initial (i.e., before mixing) optical density (A_0) of the diluted cell suspensions, 0.400 mL of each diethyl

ether (Acros Organics, Geel, Belgium) or hexane (Acros Organics, Geel, Belgium) was added to separate 2.400 mL aliquots of cell suspension. All mixtures were left to stand at room temperature for 10 min and subsequently vortexed for 1 min. The mixtures were again left to stand at room temperature for 20 min to allow phase separation of the aqueous and solvent phases, after which the optical density of the aqueous phase was measured. The affinity to each solvent was calculated using Equation 1.

$$\mathrm{Aff}_{\mathrm{solvent}} = 100 \cdot \left(1 - \frac{\mathrm{A}}{\mathrm{A}_0}\right) \quad (1)$$

With $\mathrm{Aff}_{\mathrm{solvent}}$ the affinity to a certain solvent; A, the optical density of the aqueous phase after mixing and settling; and A_0, the optical density of the cell suspension before mixing. All optical densities were measured at 400 nm in a multiwell plate, using a VersaMax tunable microplate reader (Molecular Devices, Wokingham, UK). To each well, 250 µL of (aqueous) cell suspension was added. All experiments were performed independently in duplicate.

4.6 Statistical analysis

Significant differences between the solvent affinities of the different *L. monocytogenes* strains and the strain cocktail were determined using analysis of variance (ANOVA, single variance) test at a 95.0% confidence level ($\alpha = 0.05$). Fisher's Least Significant Difference (LSD) test was used to distinguish which means were significantly different from others. Standardised skewness and standardised kurtosis were used to assess if data sets came from normal distributions. The analyses were performed using Statgraphics Centurion 18 Package (Statistical Graphics, Washington, USA). Test statistics were regarded as significant when $P \leq 0.05$.

5 CONCLUSIONS

Microscopic (CLSM) growth experiments in fish-based food model systems with different microstructures (i.e., liquid, xanthan, aqueous gel, emulsion, gelled emulsion) revealed that the growth morphology and the preferred phase for cell growth of *L. monocytogenes* were more complex than commonly assumed in macroscopic growth studies. Bacteria appeared as a combination of single cells, small aggregates and micro-colonies of different sizes, with the distribution over these categories being dependent on specific microstructural aspects of the respective model systems. This observation contradicts the traditional classification of planktonic growth in liquid/viscous systems and submerged colony growth in gelled systems. In emulsion and gelled emulsion systems, *L. monocytogenes* did not exclusively grow in the aqueous phase, but also around the fat droplets on the fat-water interface, a trend which became more evident with increasing fat content. This preference for the fat-water interface most probably was not caused by a hydrophobic cell surface of the *Listeria* strains used, and the phenomenon should be further elucidated in future studies. Previously suggested causes for differences in microbial growth parameters (i.e., the lag phase duration λ and the maximum specific growth rate μ_{max}), based on macroscopic growth experiments, were validated or rejected by means of observations at the microscopic level concerning, e.g., growth morphology, micro-colony size, inter-colony separation distances, and the preferred phase for cell growth. The occurrence of micro-colony growth in liquid/viscous foods on the one hand, and growth on the fat-water interface in (gelled) emulsion type foods on the other, could entail significant food safety implications. Under these conditions, pathogens potentially exhibit increased resistance to common food preservation techniques (e.g., thermal inactivation). Hence, this study demonstrated that combining experiments at

660 the micro- and macroscale could be beneficial for the acquirement of increased insight
661 into the food microstructural influence on microbial dynamics, concurrently leading to
662 improved food safety.
663
664

6 ACKNOWLEDGEMENTS

This work was supported by the Norconserv Foundation, FWO Vlaanderen (grant G.0863.18) and the KU Leuven Research Fund (Center of Excellence OPTEC-Optimization in Engineering and project C24/18/046).

7 REFERENCES

1. Cusack LK, Smit E, Kile ML, Harding AK. 2017. Regional and temporal trends in blood mercury concentrations and fish consumption in women of child bearing age in the united states using NHANES data from 1999-2010. Environ Health 16:10.
2. Nebeský V, Policar T, Blechna M, Křišťan J, Svačina P. 2016. Trends in import and export of fishery products in the Czech Republic during 2010-2015. Aquacult Int 24:1657-1668.
3. Nguyen TT, Hoang MV. 2018. Non-communicable diseases, food and nutrition in Vietnam from 1975 to 2015: the burden and national response. Asia Pac J Clin Nutr 27:19-28.
4. Alhassan A, Young J, Lean MEJ, Lara J. 2017. Consumption of fish and vascular risk factors: A systematic review and meta-analysis of intervention studies. Atherosclerosis 266:87-94.
5. Domingo JL. 2016. Nutrients and chemical pollutants in fish and shellfish. Balancing health benefits and risks of regular fish consumption. Crit Rev Food Sci Nutr 56(6):979-988.
6. Smith KM, Sahyoun NR. 2005. Fish consumption: Recommendations versus advisories, can they be reconciled? Nutr Rev 63(2):39-46.
7. EFSA (European Food Safety Authority), ECDC (European Centre for Disease Prevention and Control). 2017. The European Union Summary Report on trends and sources of zoonoses, zoonotic agents and food-borne Outbreaks in 2016. EFSA Journal 2017 15(12):5077.
8. Ben Embarek PK. 1994. Presence, detection and growth of *Listeria monocytogenes* in seafoods: a review. Int J Food Microbiol 23:17-34.

9. Handa S, Kimura B, Takahashi H, Koda T, Hisa K, Fujii T. 2005. Incidence of *Listeria monocytogenes* in raw seafood products in Japanese retail stores. J Food Prot 68(2):411-415.
10. Lorber B. 1997. Listeriosis. Clin Infect Dis 24:1-11.
11. Jones D. 1990. Foodborne listeriosis. Lancet 336:1171-1174.
12. McMeekin TA, Olley J, Ratkowsky DA, Ross T. 2002. Predictive microbiology: towards the interface and beyond. Int J Food Microbiol 73:395-407.
13. Van Impe JF, Poschet F, Geeraerd AH, Vereecken KM. 2005. Toward a novel class of predictive microbial growth models. Int J Food Microbiol 100:97-105.
14. Dens EJ, Van Impe JF. 2001. On the need for another type of predictive model in structured foods. Int J Food Microbiol 64:247-260.
15. Noriega E, Laca A, Díaz M. 2010. Decisive role of structure in food microbiological colonization and implications for predictive microbiology. J Food Prot 73:938-951.
16. Pin C, Sutherland JP, Baranyi J. 1999. Validating predictive models of food spoilage organisms. J Appl Microbiol 87:491-499.
17. Heertje I. 1993. Structure and function of food products. Food Struct 12:343-364.
18. Dodd C, Waites WM. 1991. The use of toluidine for in situ detection of microorganisms in foods. Lett Appl Microbiol 13:220-223.
19. Robins MM, Wilson PDG. 1994. Food structure and microbial growth. Trends Food Sci Technol 5:289-293.
20. Wang X, Devlieghere F, Geeraerd A, Uyttendaele M. 2017. Thermal inactivation and sublethal injury kinetics of *Salmonella enterica* and *Listeria*

721 *monocytogenes* in broth versus agar surface. Int J Food Microbiol 243:70-77.
722 21. Parker ML, Brocklehurst TF, Gunning PA, Coleman HP, Robins MM. 1995.
723 Growth of food-borne pathogenic bacteria in oil-in-water emulsions: I
724 Methods for investigating the form of growth of bacteria in model oil-in-water
725 emulsions and dairy cream. J Appl Bacteriol 78:601-608.
726 22. Verheyen D, Bolívar A, Pérez-Rodríguez F, Baka M, Skåra T, Van Impe JF.
727 2018. Effect of food microstructure on growth dynamics of *Listeria*
728 *monocytogenes* in fish-based model systems. Int J Food Microbiol 283:7-13.
729 23. Koutsoumanis KP, Kendall PA, Sofos JN. 2004. A comparative study on
730 growth limits of *Listeria monocytogenes* as affected by temperature, pH and
731 a_w when grown in suspension or on a solid surface. Food Microbiol 21:415-
732 422.
733 24. Noriega E, Laca A, Díaz M. 2008. Modelling of diffusion–limited growth to
734 predict *Listeria* distribution in structured model foods. J Food Eng 87:247-256.
735 25. Theys TE, Geeraerd AH, Verhulst A, Poot K, Van Bree I, Devlieghere F,
736 Moldenaers P, Wilson D, Brocklehurst T, Van Impe JF. 2008. Effect of pH,
737 water activity and gel micro-structure, including oxygen profiles and
738 rheological characterization, on the growth kinetics of *Salmonella*
739 Typhimurium. Int J Food Microbiol 128:67-77.
740 26. Wilson PDG, Brocklehurst TF, Arino S, Thuault D, Jakobsen M, Lange M,
741 Farkas J, Wimpenny JWT, Van Impe JF. 2002. Modelling microbial growth in
742 structured foods: towards a unified approach. Int J Food Microbiol 73:275-
743 289.
744 27. Wimpennny JWT, Coombs JP. 1983. Penetration of oxygen into bacterial
745 colonies. J Gen Microbiol 129:1239-1242.

28. Baka M, Noriega E, Van Langendonck K, Van Impe JF. 2016. Influence of food intrinsic complexity on *Listeria monocytogenes* growth in/on vacuum-packed model systems at suboptimal temperatures. Int J Food Microbiol 235:17-27.

29. Baka M, Vercruyssen S, Cornette N, Van Impe JF. 2017. Dynamics of *Listeria monocytogenes* at suboptimal temperatures in/on fish-protein based model systems: Effect of (micro)structure and microbial distribution. Food Control 73:43-50.

30. Baka M, Verheyen D, Cornette N, Vercruyssen S, Van Impe JF. 2017. *Salmonella* Typhimurium and *Staphylococcus aureus* dynamics in/on variable (micro)structures of fishbased model systems at suboptimal temperatures. Int J Food Microbiol 240:32-39.

31. Verheyen D, Baka M, Glorieux S, Duquenne B, Fraeye I, Skåra T, Van Impe JF. 2018. Development of fish-based model systems with various microstructures. Food Res Int 106:1069-1076.

32. Baranyi J, Roberts TA. 1994. A dynamic approach to predicting bacterial growth in food. Int J Food Microbiol 23:277-294.

33. Jeanson S, Floury J, Gagnaire V, Lortal S, Thierry A. 2015. Bacterial colonies in solid media and foods: A review on their growth and interactions with the micro-environment. Front Microbiol 6:1264.

34. Dos Reis-Teixeira FB, Alves VF, De Martinis ECP. 2017. Growth, viability and architecture of biofilms of *Listeria monocytogenes* formed on abiotic surfaces. Braz J Microbiol 48:587-591.

35. Bae E, Bai N, Aroonnual A, Bhunia AK, Hirleman ED. 2011. Label-free identification of bacterial microcolonies via elastic scattering. Biotechnol

771 Bioeng 108:637-644.
772 36. Choo-Smith LP, Maquelin K, van Vreeswijk T, Bruining HA, Puppels GJ,
773 Ngo Thi NA, Kirschner C, Naumann D, Ami D, Villa AM, Orsini F, Doglia
774 SM, Lamfarraj H, Sockalingum GD, Manfait M, Allouch P, Endtz HP. 2001.
775 Investigating microbial (micro)colony heterogenity by vibrational
776 spectroscopy. Appl Environ Microbiol 67(4):1461-1469.
777 37. Zhao Y, Knøchel S, Siegumfeldt H. 2014. *In situ* examination of *Lactobacillus*
778 *brevis* after exposure to an oxidizing disinfectant. Front Microbiol 5:635.
779 38. Boons K, Mertens L, Van Derlinden E, David CC, Hofkens J, Van Impe JF.
780 2013. Behavior of *Escherichia coli* in a Heterogeneous Gelatin-Dextran
781 Mixture. Appl Environ Microbiol 79(9):3126-3128.
782 39. Paddock SW. 1999. An introduction to confocal imaging, p 43–56. In Paddock
783 SW (ed), Methods in Molecular Biology, vol. 122: Confocal Microscopy
784 Methods and Protocols. Humana Press Inc., Totowa, NJ.
785 40. Bellon-Fontaine MN, Rault J, van Oss, CJ. 1996. Microbial adhesion to
786 solvents: a novel method to determine the electron-donor/electron-acceptor or
787 Lewis acid-base properties of microbial cells. Colloids Surf B Biointerfaces
788 7:47-53.
789 41. Russ JC. 2005. Image analysis of food microstructure. CRC Press LLC, Boca
790 Raton, FL.
791 42. Jung JH, Lee JE. 2016. Real-time bacterial microcolony counting using on-
792 chip microscopy. Sci Rep 6:21473
793 43. Holt JG, Krieg NR, Sneath PHA, Staley JT, Williams ST. 1994. Bergeys
794 Manual of Determinative Bacteriology, 9th ed. Williams, Wilkins, Baltimore.
795 44. Melaugh G, Hutchison J, Kragh KN, Irie Y, Roberts A, Bjarnsholt T, Diggle

SP, Gordon, VD, Allen, RJ. 2016. Shaping the growth behaviour of biofilms initiated from bacterial aggregates. PLoS ONE 11(3): e0149683.

45. Smet C, Noriega E, Van Mierlo J, Valdramidis VP, Van Impe JF. 2015a. Influence of the growth morphology on the behavior of *Salmonella* Typhimurium and *Listeria monocytogenes* under osmotic stress. Food Res Int 77:515-526.

46. Smet C, Van Derlinden E, Mertens L, Noriega E, Van Impe JF. 2015b. Effect of cell immobilization on the growth dynamics of *Salmonella* typhimurium and *Escherichia coli* at suboptimal temperatures. Int J Food Microbiol 208:75-83.

47. Malakar PK, Brocklehurst TF, MacKie AR, Wilson PDG, Zwietering MH, van't Riet K. 2000. Microgradients in bacterial colonies: use of flueorescence ratio imaging, a non-invasive technique. Int J Food Microbiol 56:71-80.

48. Brocklehurst TF, Wilson PDG. 2000. The role of lipids in controlling microbial growth. Grasas y aceites 51:66-73.

49. Prachaiyo P, McLandsborough LA. 2003. Oil-in-water emulsion as a model system to study the growth of *Escherichia coli* O157:H7 in a heterogeneous food system. J Food Sci 68(3):1018-1024.

50. Peng K, Liu W, Xiong Y, Lu L, Liu J, Huang X. 2018. Emulsion microstructural evolution with the action of environmentally friendly demulsifying bacteria. Colloids Surf A 553:528-538.

51. Wen, Y, Cheng, H, Lu, LJ, Liu J, Feng Y, Guan W, Zhou Q, Huang XF. 2010. Analysis of biological demuslification process of water-in-oil emulsion by *Alcaligenes* sp. S-XJ-1. Bioresour Technol 101:8315-8322.

52. Xiong Y, Huang X, Liu J, Lu L, Peng K. 2018. Preparation of magnetically

responsive bacterial demulsifier with special surface properties for efficient demulsification of water/oil emulsion. Renew Energy 129:786-793.

53. Lopez C, Maillard MB, Briard-Bion V, Camier B, Hannon JA. 2006. Lipolysis during ripening of Emmental cheese considering organization of fat and preferential localization of bacteria. J Agric Food Chem 54:5855-5867.

54. Gorski L, Duhé JM, Flaherty D. 2009. The use of flagella and motility for plant colonization and fitness by different strains of the foodborne pathogen *Listeria monocytogenes*. PLoS ONE 4(4):e5142.

55. Ron EZ. 2000. Microbial life on petroleum, p 303–316. In Seckbach J (ed), Journey to diverse microbial worlds: Adaptation to exotic environments. Kluwer Academic Publishers., Dordrecht, The Netherlands.

56. Peel M, Donachie W, Shaw A. 1988. Temperature-dependent expression of flagella of *Listeria monocytogenes* studied by electron microscopy, SDS-PAGE and western blotting. J Gen Microbiol 134:2171-2178.

57. Mattila M, Lindström M, Somervuo P, Markkula A, Korkeala H. 2011. Role of flhA and motA in growth of *Listeria monocytogenes* at low temperatures. Int J Food Microbiol 148:177-183.

58. Caly D, Takilt V, Lebret V, Tresse O. 2009. Sodium chloride affects *Listeria monocytogenes* adhesion to polystyrene and stainless steel by regulating flagella expression. Lett. Appl. Microbiol 49:751-756.

59. Tresse O, Lebret V, Benezech T, Faille C. 2006. Comparative evaluation of adhesion, surface properties and surface protein composition of *Listeria monocytogenes* strains after cultivation at constant pH of 5 and 7. J Appl Microbiol 101:53-62.

60. Takahashi H, Suda T, Tanaka Y, Kimura B. 2010. Cellular hydrophobicity of

Listeria monocytogenes involves initial attachment and biofilm formation on the surface of polyvinyl chloride. Lett Appl Microbiol 50:618-625.

61. Briandet R, Meylheuc T, Maher C, Bellon-Fontaine MN. 1999. *Listeria monocytogenes* Scott A: Cell surface charge, hydrophobicity, and electron donor and acceptor characteristics under different environmental growth conditions. Appl Environ Microbiol 65(12):5328-5333.
62. Chavant P, Martinie B, Meylheuc T, Bellon-Fontaine MN, Hebraud M. 2002. *Listeria monocytogenes* LO28: Surface physicochemical properties and ability to form biofilms at different temperatures and growth phases. Appl Environ Microbiol 68(2):728-737.
63. Szlavik J, Paiva DS, Mørk N, van den Berg F, Verran J, Whitehead K, Knøchel S, Nielsen DS. 2012. Initial adhesion of *Listeria monocytogenes* to solid surfaces under liquid flow. Int J Food Microbiol 152:181-188.
64. Bernbom N, Jørgensen RL, Ng YY, Meyer RL, Kingshott P, Vejborg RM, Klemm P, Besenbacher F, Gram L. 2006. Bacterial adhesion to stainless stell is reduced by aqueous fish extract coatings. Biofilms 3:26-36.
65. Goulter RM, Gentle IR, Dykes GA. 2009. Issues in determining factors influencing bacterial attachment: a review using the attachment of *Escherichia coli* to abiotic surfaces as an example. Lett Appl Microbiol 49:1-7.
66. Thomas LV, Wimpenny JWT, Barker GC. 1997. Spatial interactions between subsurface bacterial colonies in a model system: a territory model describing the inhibition of *Listeria monocytogenes* by a nisin-producing lactic acid bacterium. Microbiology 143:2575-2582.
67. Wimpenny JWT, Leistner L, Thomas LV, Mitchell AJ, Katsaras K, Peetz P. 1995. Submerged bacterial colonies within food and model systems, their

growth, distribution and interactions. Int J Food Microbiol 28:299-315.

68. Skandamis PN, Jeanson S. 2015. Colonial vs. planktonic type of growth: mathematical modeling of microbial dynamics on surfaces and in liquid, semi-liquid and solid foods. Front Microbiol 6:1178.

69. Mossel DAA, Cony JEL, Struijk CB, Baird RM. 1995. Essentials of the Microbiology of Foods.. Wiley, West Sussex, UK.

70. Smet C, Noriega E, Rosier F, Walsh JL, Valdramidis VP, Van Impe JF. 2017. Impact of food model (micro)structure on the microbial inactivation efficacy of cold atmosperic plasma. Int J Food Microbiol 240:47-56.

71. Frost I, Smith WPJ, Mitri, S, San Millan A, Davit Y, Osborne JM, Pitt-Francis JM, Maclean RC, Foster KR. 2018. Cooperation, competition and antibiotic resistance in bacterial colonies. ISME J 12:1582-1593.

72. Aquerreta Y, Astiasarán I, Mohino A, Bello J. 2002. Composition of pâtés with mackerel flesh (*Scomber scombrus*) and tuna liver (*Thunnus thynnus*): comparison with commerical fish pâtés. Food Chem 77:147-153.

73. Echarte M, Conchillo A, Ansorena D, Astiasarán I. 2004. Evaluation of the nutritional aspects and cholesterol oxidation products of pork liver and fish patés. Food Chem 86:47-53.

74. Ahmed EO, Elhaj GA. 2011. The chemical composition, microbiological detection and sensory evaluation of fresh fish sausage made from *Clarias lazera* and *Tetradon fahaka*. J Fish Aquaculture 2(1):11-16.

75. Andersen JB, Roldgaard BB, Lindner AB, Christensen BB, Licht TR. 2006. Construction of a multiple fluorescence labelling system for use in co-invasion studies of *Listeria monocytogenes*. BMC Microbiol 6:86.

76. Kankaanpää P, Paavolainen L, Tiitta S, Karjalainen M, Päivärinne J, Nieminen

J, Marjomäki V, Heino J, White DJ. 2012. BioImageXD: an open, general-purpose and high-throughput image-processing platform. Nat Methods 9(7):683-689.

TABLES

Table 1: Affinity to diethyl ether and hexane of the four different tested *Listeria monocytogenes* strains and the strain cocktail consisting of LMG 23773, LMG 23774 and LMG 26484, according to the MATS (Microbial Adhesion To Solvents) assay. Among the four different strains and the strain cocktail, solvent affinity values bearing different uppercase letters are significantly different ($P \leq 0.05$). For each strain, affinity values to the different solvents bearing different lowercase letters are significantly different ($P \leq 0.05$).

	$Aff_{diethyl\ ether}$ (%)	Aff_{hexane} (%)
LMG 23773	$53.66 \pm 9.11^{B,b}$	$8.64 \pm 2.35^{B,a}$
LMG 23774	$34.25 \pm 5.69^{A,b}$	$-5.54 \pm 2.38^{A,a}$
LMG 26484	$29.73 \pm 5.45^{A,b}$	$0.52 \pm 4.56^{AB,a}$
GFP strain	$30.16 \pm 3.06^{A,b}$	$10.83 \pm 6.05^{B,a}$
Strain cocktail	$30.25 \pm 5.94^{A,b}$	$-2.34 \pm 4.41^{A,a}$

Table 2: Statistical analysis of macroscopic growth parameters (lag phase λ and maximum specific growth rate μ_{max}) for the *L. monocytogenes* strain cocktail consisting of LMG 23773, LMG 23774 and LMG 26484, according to the Baranyi and Roberts (1994) model. For the different model systems at the same temperature, parameter values bearing different uppercase letters are significantly different ($P \leq 0.05$). Adapted from Verheyen et al. (22).

Model system	λ (h)		μ_{max} (1/h)	
	4°C	10°C	4°C	10°C
Liquid	124.2±6.3^{C}	14.0±7.2^{A}	0.029±0.001^{B}	0.091±0.004^{B}
Xanthan	89.5±12.6^{B}	16.2±4.2^{A}	0.029±0.001^{B}	0.101±0.003^{C}
Aqueous gel	93.3±11.0^{B}	28.5±6.2^{A}	0.026±0.001^{A}	0.074±0.003^{A}
Emulsion (1%)	45.0±10.0^{A}	19.2±6.4^{A}	0.031±0.001^{C}	0.094±0.004^{B,C}
Gelled emulsion (1%)	53.6±13.7^{A}	21.1±7.2^{A}	0.029±0.001^{B}	0.079±0.003^{A}

FIGURE CAPTIONS

Figure 1: Number distribution (%) of single cells, small aggregates, and micro-colonies with different sizes for the GFP *L. monocytogenes* strain after 14 days of growth at 10°C in the 11 model systems, i.e., Liquid, Xanthan, Aqueous gel, Emulsions (Em) with 4 different fat contents, and Gelled emulsions (GE) with 4 different fat contents. Micro-colony sizes (µm) are expressed in terms of the equivalent spherical radius (r_s).

Figure 2: Volume distribution (%) of single cells, small aggregates, and micro-colonies with different sizes for the GFP *L. monocytogenes* strain after 14 days of growth at 10°C in the 11 model systems, i.e., Liquid, Xanthan, Aqueous gel, Emulsions (Em) with 4 different fat contents, and Gelled emulsions (GE) with 4 different fat contents. Micro-colony sizes (µm) are expressed in terms of the equivalent spherical radius (r_s).

Figure 3: Growth of *L. monocytogenes* in the liquid (A), xanthan (B), and aqueous gel (C) model systems. Cells are depicted in green.

Figure 4: Growth of *L. monocytogenes* in the emulsion (A) and gelled emulsion (B) model systems with a fat content of 1%. Cells are depicted in green, while fat droplets are depicted in orange. Yellow areas represent *L. monocytogenes* growth on the fat-water interphase.

Figure 5: Growth of *L. monocytogenes* in the emulsion model systems with different fat content, i.e., 5% (A), 10% (B), and 20% (C). Cells are depicted in

green, while fat droplets are depicted in orange. Yellow areas represent *L. monocytogenes* growth on the fat-water interphase.

Figure 6: Growth of *L. monocytogenes* in the gelled emulsion model systems with different fat content, i.e., 5% (A), 10% (B), and 20% (C). Cells are depicted in green, while fat droplets are depicted in orange. Yellow areas represent *L. monocytogenes* growth on the fat-water interphase.

Applied and Environmental Microbiology

AEM

Applied and Environmental Microbiology

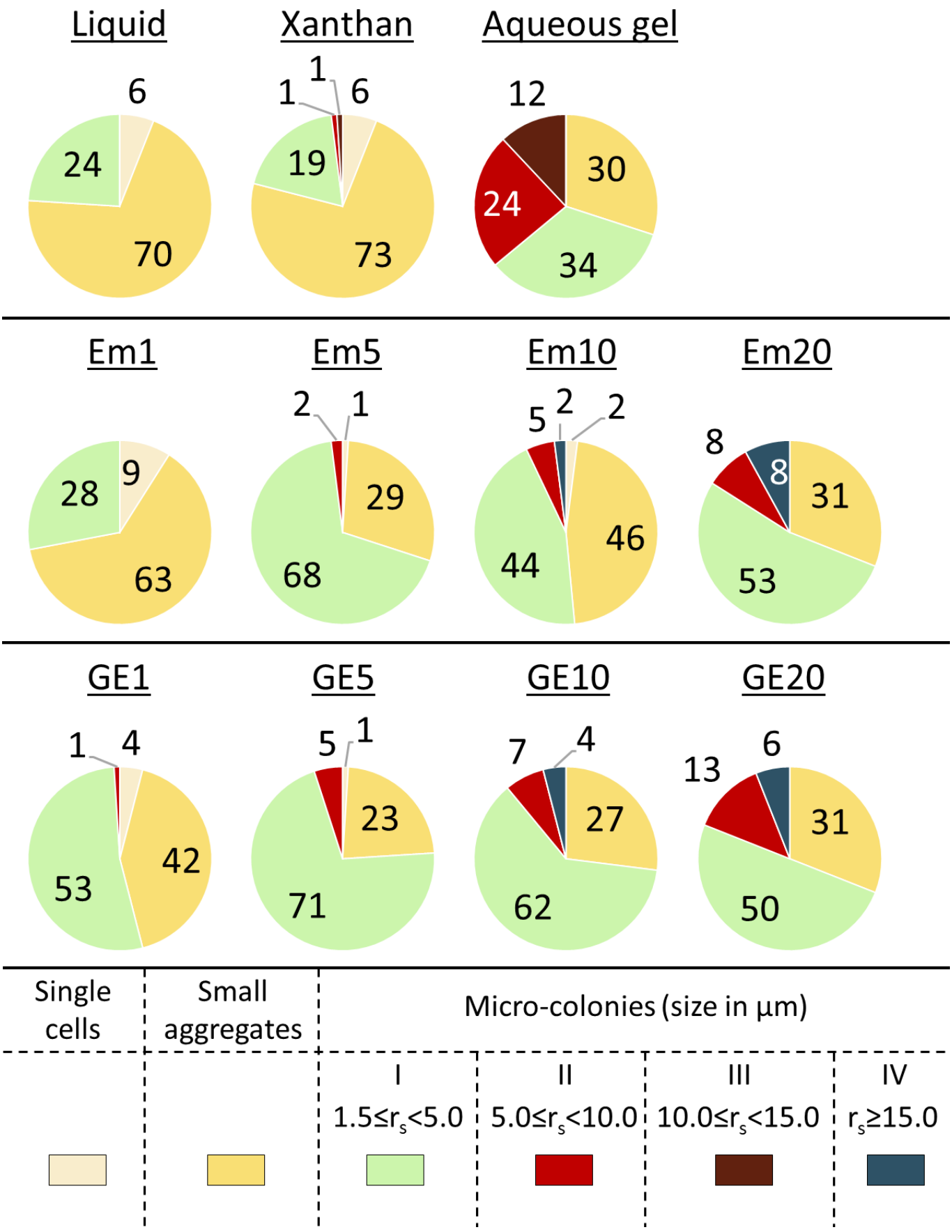

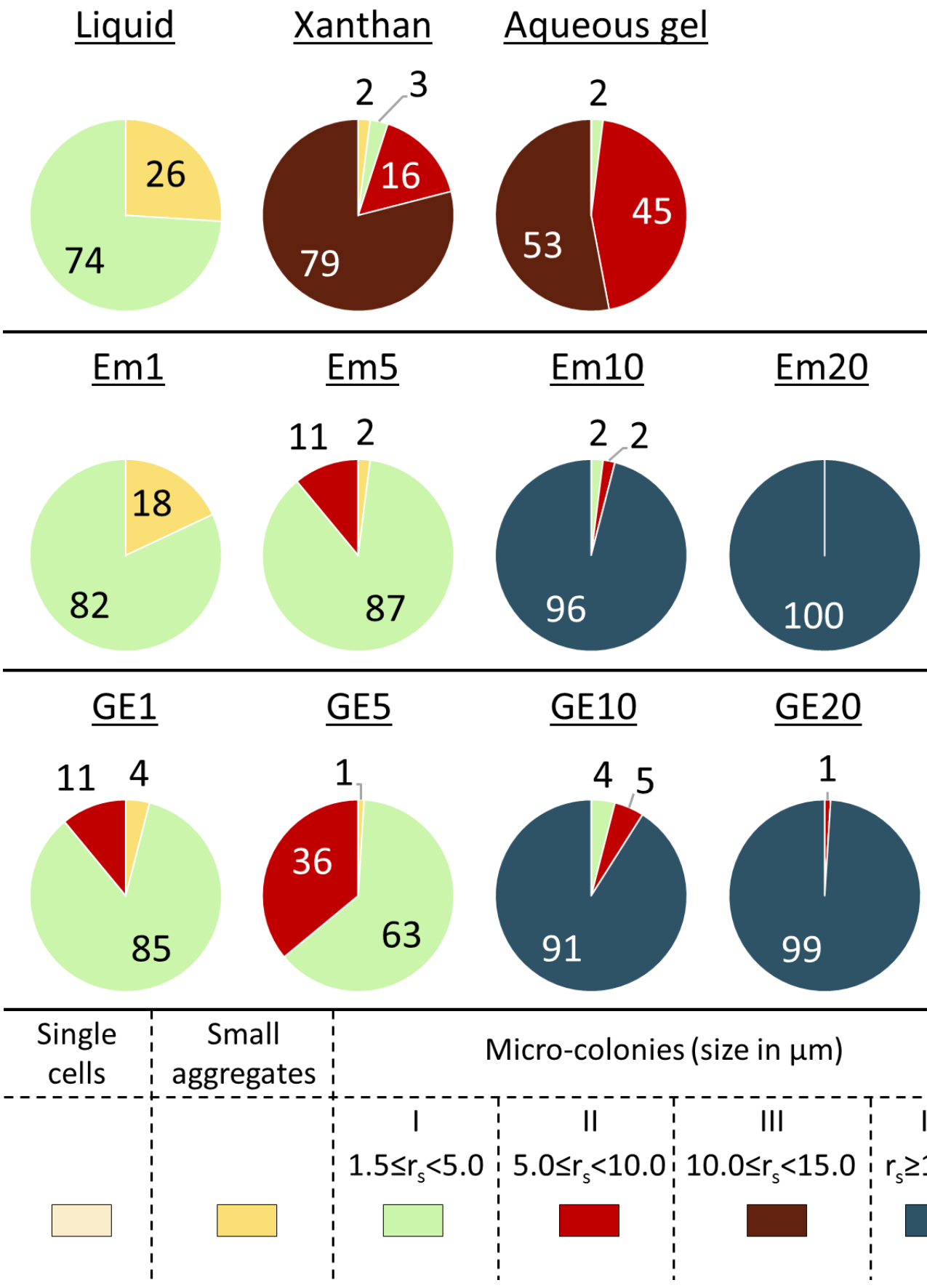

Applied and Environmental Microbiology

AEM

Applied and Environmental Microbiology

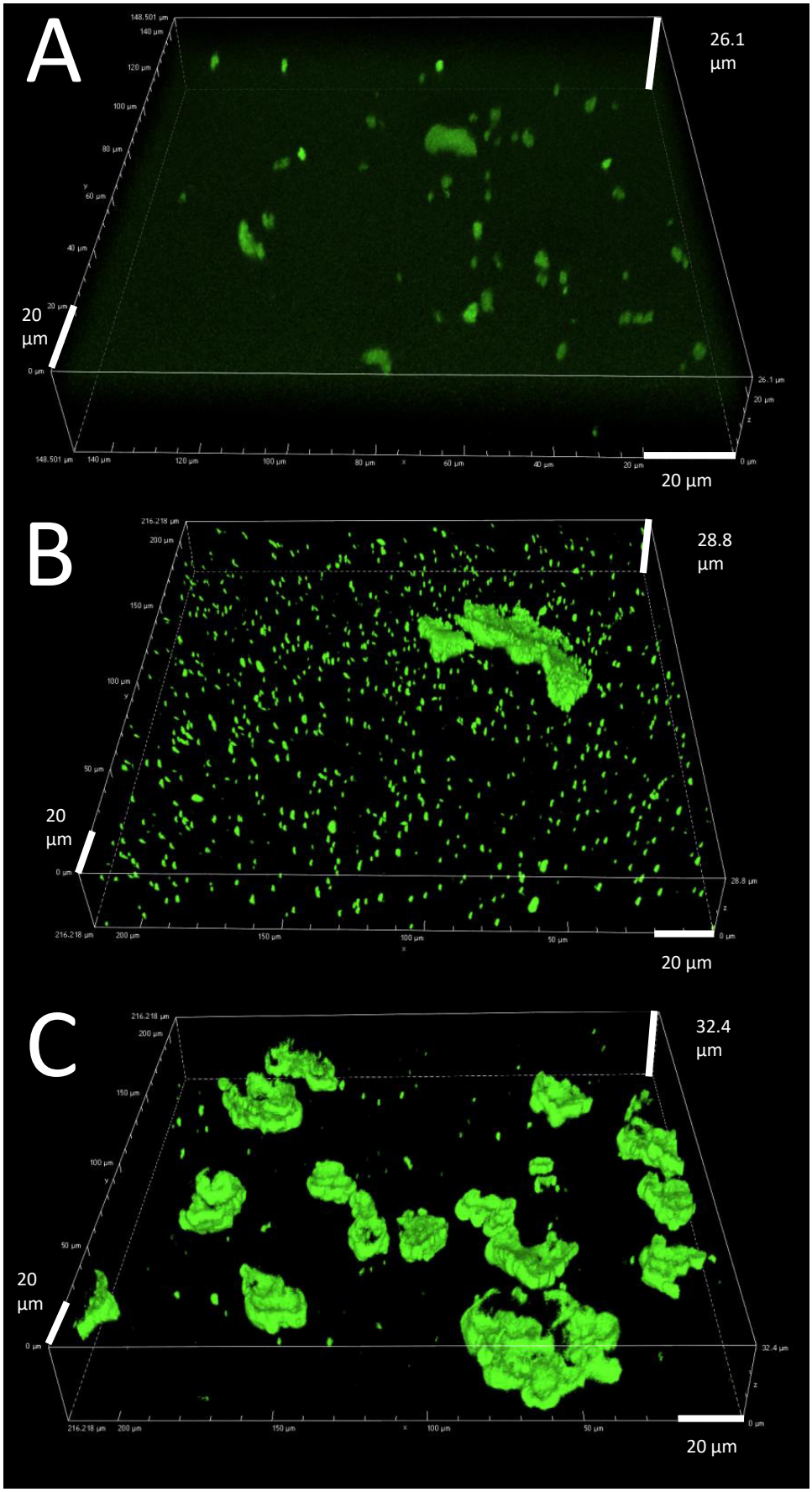

Applied and Environmental Microbiology

AEM

Applied and Environmental Microbiology